DEVELOPMENT OF AN ACCELERATED DEGRADATION TESTBED FOR INTEGRATED VIBRATION MONITORING AND ONLINE OIL ANALYSIS OF VEHICLE DIFFERENTIAL BEARINGS

Cody M. Walker, Alec B. Salakovich, David K. Irick, Jamie B. Coble, and Cyrus Smith
Nuclear Engineering
Mechanical, Aerospace, and Biomedical Engineering
PYA Analytics
University of Tennessee, Knoxville
Nuclear Engineering Department
421 Nuclear Engineering Building
Knoxville, TN 37996
Telephone: (931) 797-5403
Email: cwalke42@utk.edu

Abstract: This project, sponsored by the Office of Naval Research, integrates oil and vibration analysis to develop a more complete diagnostic and prognostic model for monitoring bearing degradation and performance in the field. The results of this project will be used to optimize repair schedules and minimize the risk of catastrophic failure of machine components for military personnel during a mission through enhanced condition-based maintenance. Each test bearing is first introduced with an outer race fault. The fault's degradation is accelerated by running the bearing under overloaded conditions in the boundary lubrication regime within a large test rig designed for these conditions. Accumulated damage to the bearing is characterized in another clean, low-noise test rig to collect vibration signatures. Finally, the bearing is implemented into the differential for in-situ testing to emulate data in the field. Dynamic characterization of the designed test machines was performed by long runs spanning multiple hours under rated conditions to determine any wear-in effects and ramp-up tests to distinguish order-based bearing frequencies and structural resonances. Modal analyses were performed on the static system to provide additional evidence of structural resonances within the machines. This paper will discuss the design challenges and solutions for creating a test bed to monitor bearings in accelerated-degradation conditions and in realistic operating conditions.

Key words: Bearings; boundary lubrication; diagnostics; frequency response function; health monitoring; prognostics;

Introduction:

Bearing are an integral component to most power transport devices including motors, drive fans, compressors, pumps and conveyors. Bearing fault diagnostics typically rely on vibration analysis to identify defects located on the bearing's inner race, outer race, rolling

element, or cage. Bearing vibration analysis is used to determine the type of fault, if any, that is present, estimate the size of the fault or defect, and calculate the remaining useful life (RUL) of that component.

Prognostics aim to minimize in-use component failures by calculating the remaining useful life of essential components. Prognostic modeling requires run-to-failure data, but many industries replace their systems at the first indication of a fault. For example, a reactor coolant pump should not be run-to-failure while in the system. This is why run-to-failure data is a premium. There are few sources of such data for prognostics data sets. The National Aeronautics and Space Administration has set up a prognostics data repository to allow the exchange of publicly available data sets to work with (Administration 2019). Some industries, such as paper mills, have systems where faults develop slowly over months and even years (James C. Robinson 2018). Exactly recreating such faults in a laboratory setting would not be time efficient. Accelerated degradation testing provides realistic run-to-failure data for each stages of degradation seen in these systems, while reducing the time required to days or weeks (Nectoux et al. 2012). This is accomplished by overstressing the component of interest. By running under boundary lubrication rather than full fluid-film lubrication, the sliding friction between the rollers and the races increases. Boundary lubrication occurs when the lubrication layer is so thin that its viscosity no longer plays a significant role in the friction coefficient (Snow 2001). The lubricant and the nature of the surface determine the friction coefficient. When boundary lubrication exists, frictional wear increases and the lubrication can become contaminated with wear particles as the high spots of surfaces come into contact (Snow 2001). This type of friction will accelerate the degradation of the bearing and reduce its overall life. By understanding how the bearings degrade, maintenance can be scheduled based on the condition of the bearing rather replacing them at arbitrary intervals.

Condition-based maintenance is implemented in the military-based programs such as the System Health Management (SHM) program and its subset the Health and Usage Monitoring Systems (HUMS) toolkit (Team 2013). These initiatives have attempted to utilize existing or add-on steady state sensors for both diagnostics and prognostics. The SHM programs improve safety, increase reliability, and enhance situational awareness for crews. It is imperative that Humvees and helicopters do not burn out mid-mission as the consequences could be far worse than just loss of revenue. This project is working towards monitoring bearings within the differential of wheeled land vehicles. Run-to-failure data can be produced by seeding the bearings with faults then degrading them under accelerated conditions. The ultimate goal of this research is to provide early warning of incipient faults and accurate prognosis of failures throughout the component life.

The Bearing Test Rig was designed to assess the vibrational characteristics of a damaged bearing in a low-noise environment before taking measurements in the differential where it is used. The differential is likely to have a far noisier environment due to the extensive inner workings. Characterizing the damage with a low-noise rig will provide measurements that will be used to help distinguish the bearing fault frequencies from other vibrations

within the differential. While the test rig is a low-noise environment, it is still not without its own characteristics that will show up in the measurements. Structural resonances of the test rig were investigated via impact hammer testing to develop a frequency response function (FRF). Such testing is important as the cyclical inputs provided by the shaft and bearings may excite natural frequencies of the structure and such resonances can cause unrealistically high magnitudes at bearing fault frequencies. The Bearing Test Rig was placed onto isolation pads to decouple the rig from the table that it rests on. Without the isolation pads, the table will resonate in response to the Bearing Test Rig's vibrations causing a noisier environment. These kinds of effects can be seen with a FRF and impact hammer testing.

The natural frequency of an object describes the frequency at which an object will dissipate the energy through vibration when an excitation is introduced. A common example of this effect is when a bell or tuning fork is struck. The magnitude of the strike affects the volume of the subsequent ring-down, but the tone is a function of the structure of the object and therefore is always consistent. Structural resonances such as these are important when performing vibration analysis work. If they exist near a frequency of interest, they can resonate and amplify the vibration response, causing either damage or affecting the credibility of sensor readings.

Mathematical modeling of this phenomenon is most simply expressed by a single degree of freedom (SDOF) system. In the SDOF system, the vibration characteristics are represented using four idealized components: mass, spring, damper, and excitation. Figure 1 shows the configuration for the theoretical system.

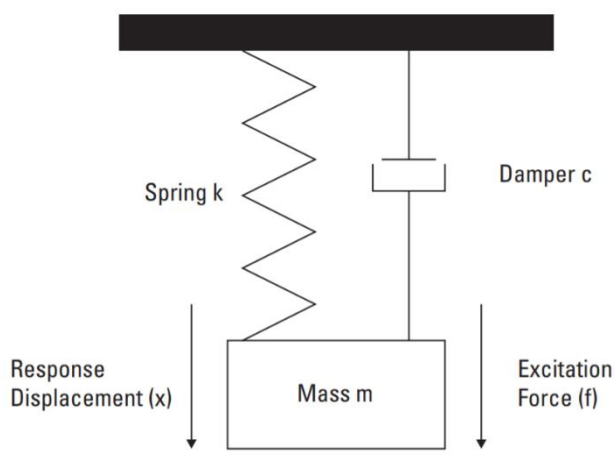

Figure 1: Configuration of Single Degree of Freedom System (Technologies 1997)

In this ideal system, the mass (m), spring constant (k), and damping constant (c) are all fixed values and the output (x) is only changed as a function of the input variable (f). The dynamics of this system are modeled by the equation of motion, shown as Equation 1.

$$\frac{d^2x(t)}{dt^2} + 2\xi\omega_n\frac{dx(t)}{dt} + {\omega_n}^2x(t) = \frac{f(t)}{m} \tag{1}$$

$$\text{where } 2\xi\omega_n = \frac{c}{m}, \omega_n{}^2 = \frac{k}{m}$$

Equation 1 is then manipulated with a Laplace transform and the ratio of the input and output, known as the transfer function, is shown in Equation 2.

$$\frac{x(s)}{f(s)} = \frac{1}{m(s^2+2\xi\omega_n s+\omega_n{}^2)} \tag{2}$$

$$\text{with roots: } s_{1,2} = -\xi\omega_n \pm \omega_n\sqrt{\xi^2-1}$$

The frequency response of the system can be plotted in polar coordinates to provide a visual representation of the system. Equations 3 and 4 show the formulas for magnitude and phase, respectively, of the response (Technologies 1997).

$$H(\omega) = \frac{1/m}{\sqrt{(\omega_n{}^2-\omega^2)^2+(2\xi\omega\omega_n)^2}} \tag{3}$$

$$\theta(\omega) = tan^{-1}\left(\frac{2\xi\omega\omega_n}{\omega_n{}^2-\omega^2}\right) \tag{4}$$

However, very few systems behave as ideally as a mass on a spring. Many structures have multiple degrees of freedom (MDOF) and exhibit many modes of excitation. Such systems are modeled as a weighted sum of multiple SDOF systems. Equation 5 shows the curve fitting function for a MDOF system.

$$H(\omega) = \sum_{r=1}^{n} \frac{\phi_r/m}{\sqrt{(\omega_n{}^2-\omega^2)^2+(2\xi\omega\omega_n)^2}} \tag{5}$$

Where ϕ_r is the modal participation factor and "is a function of excitation and mode shape coefficients at the input and output degrees of freedom (Technologies 1997)."

In order to accelerate the degradation in the bearing after characterization has been completed, operation will take place in oil-starved conditions, or more specifically, boundary lubrication. The boundary lubrication regime is where most of the load in the bearing is being supported on the asperities, or the peaks associated with the surface roughness of the interface, rather than being supported by a layer of lubrication (Hironaka 1984). Figure 2 below shows the Stribeck curve, which shows the various lubrication regimes and how the load is supported relative to the regime. In the equations shown in Figure 2, f represents the coefficient of friction, η is lubricant viscosity, V is the velocity of sliding surfaces, h is the oil film thickness and F_N is the load.

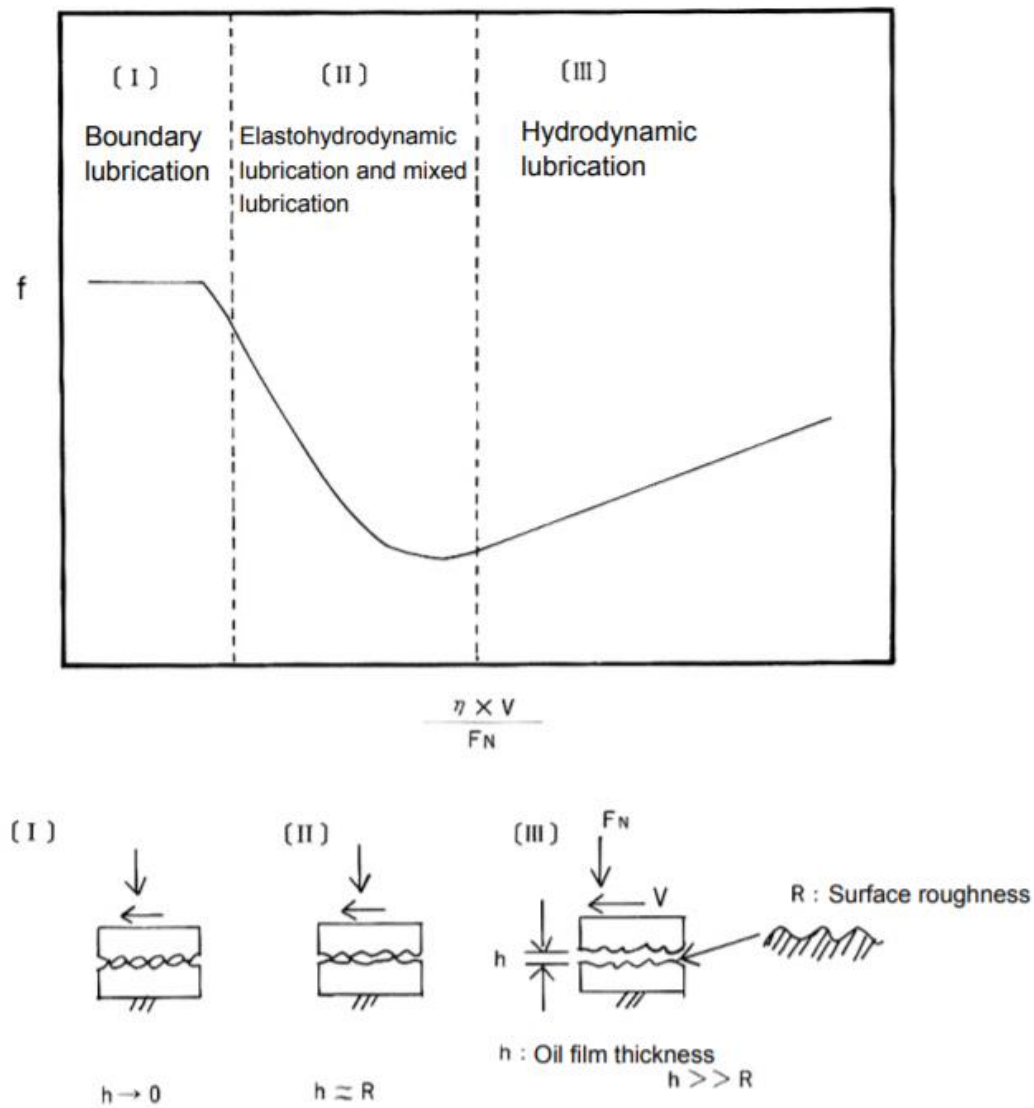

Figure 2: Stribeck Curve and Lubrication Regimes(Hironaka 1984)

Due to the higher coefficient of friction and higher temperatures acting on thinner layers of oil, oxidation reactions occur more readily within the oil. Initially, 75W-90 gear oil was intended for the tests as the chemical characteristics revealed in the oil analysis would represent the type of oil used within the differential. However, the kinematic viscosity of gear oil is 14.6 cSt at 100°C and the high viscosity makes it difficult to enter the boundary lubrication regime ('Mobil 1TM Synthetic Gear Lube LS | MobilTM Motor Oils.'). Aeroshell Turbine Oil 555 (also referred to as “triple-nickel”) was used in tests due to its far lower viscosity. Figure 3 shows the temperature-viscosity curve for various Aeroshell oils with 555 emphasized in red.

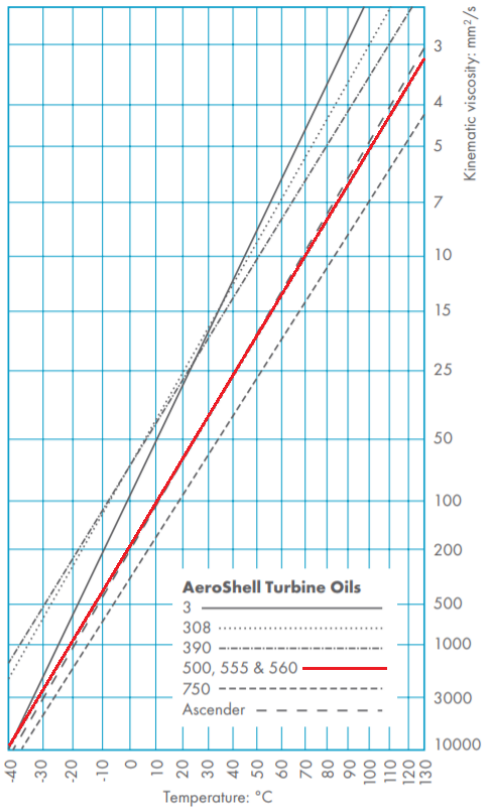

Figure 3: Typical Temperature-Viscosity Curves of Aeroshell Turbine Oils (1 cSt = 1 mm²/s)(Aeroshell Turbine Engine Oils 2012).

At 100°C, the viscosity of Aeroshell 555 is roughly one-third that of the 75W-90 gear oil. This lower viscosity results in a thinner oil layer between contact surfaces, thus making boundary lubrication more easily achieved. Requiring supervised operation, using the Aeroshell 555 reduces the time to reach boundary lubrication and more time of a single run can be used degrading the bearing.

Bearing skidding is an unintentional way to damage the bearing, which was seen at times during testing. Skidding occurs when the resistance of the roller or the cage overcomes the forward force from the inner race (Solutions 2019). This prevents the roller from adequately rolling, thus sliding. This sliding effect can form streaks and smears along the rollers and races leading to excessive pitting formation (Solutions 2019). Bearing skidding can be diagnosed through vibration analysis. It characteristically appears as an elevated noise floor in higher frequencies with protruding peaks spaced at frequencies relating to the bearing's outer or inner race fault frequency (Institute 2019). Skidding was seen in the Bearing Test Rig due a locking nut becoming loose during operation. This locking nut pressed the inner race into the rollers and outer race. Without proper compression, a small clearance formed, which allowed the rollers to skid rather than roll.

Methodology:

Three tests were used in the characterization of the Bearing Test Rig. First, impact hammer testing on the static system is used to identify structural resonances that may interfere with the collection of meaningful data through analysis of the system's response to an impulse excitation, otherwise known as the Frequency Response Function (FRF). The second test is a long run that provides a wear-in period for new bearings and gives insight into the steady state conditions achieved during extended operation. Finally, a ramp-up test that acquires a data sample at each operating frequency of interest to show how bearing and resonance frequencies move throughout the operating range. Table 1 shows the bearing defect frequencies for the bearings used in these experiments.

Table 1: Bearing Fault Frequencies (Generated from the SKF Engineering Calculator)

			Bearing Fault Frequencies (Order)			
Bearing Role	Product Number	Bearing Type	BPFI	BPFO	Cage	BSF
Test	JLM506849A	Tapered Roller	12.239	9.761	0.444	4.263
Support	7315WN	Angular Contact	7.056	4.944	0.412	2.11

Typically, data were sampled at 10,240 Hz and in the case of dynamic tests; data were sampled over 15 second intervals and all bearings were under well-lubricated conditions. The presented spectra are generated by averaging the spectra for each second within the sampling interval to minimize signal noise. The results from these tests are used to identify desirable operating conditions for data collection on bearings with known faults.

Figure 4 shows the design of the Bearing Test Rig. The Bearing Test Rig has a 3 hp motor that is controlled with a variable frequency drive (VFD). The motor is attached to a pulley, which spins the shaft. The two test bearings are located towards the ends of the shafts, while two greased-filled support bearing are closer to the pulley on the middle. The test bearings are lubricated with a once-through cycle. The oil that flows through the bearings is collected via the downward-facing spouts and will undergo further testing later. The test bearings are radially loaded with two hydraulic pumps capable of applying 20,000 lb of force. This force is applied in the same direction as the red arrows in Figure 4.

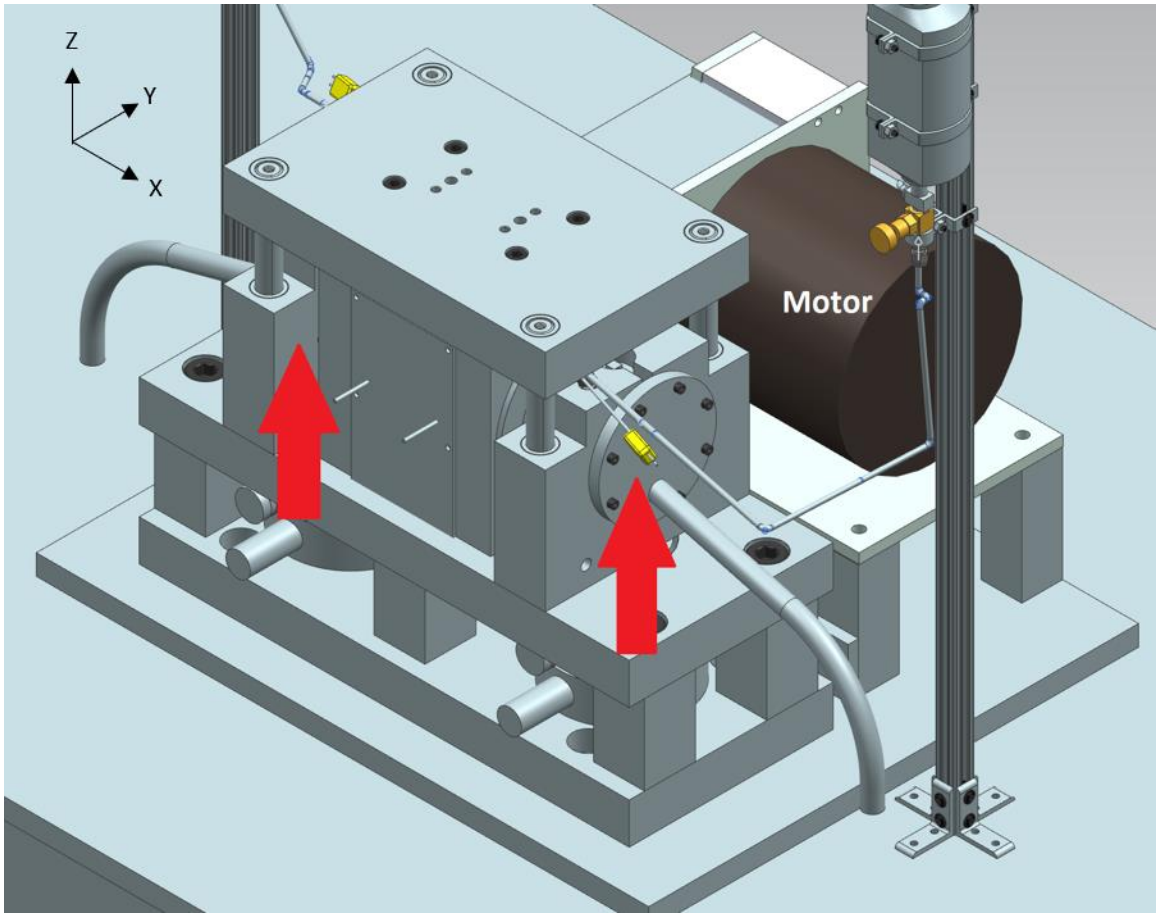

Figure 4: CAD model of the Bearing Test Rig. The red arrows indicate the location of the two test bearings.

2.1: Frequency Response Tests

To determine the frequency response function of the test rig, it was struck with an impact hammer to excite the structural resonances and the input-output relationship was recorded. When carrying out the test, the rig was struck in the same location three times with ample time between blows to allow the rig to ring down. During these periods, data were continuously collected until the final ring-down had decayed. The data were then post processed in MATLAB by choosing a window length large enough to capture the entire ringdown from each blow. The successive blows were then concatenated as shown in Figure 5 and evaluated using the "modalfrf.m" function in MATLAB, which uses Welch's averaged, modified periodogram method to estimate the frequency response function as the cross-power spectral densities of the input and output.

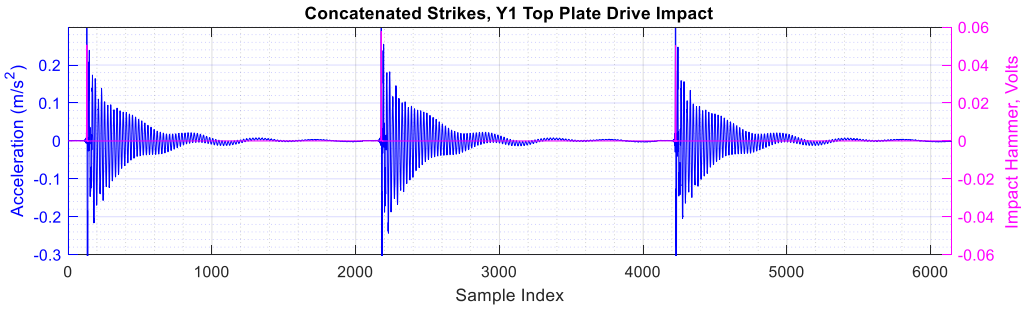

Figure 5: Preprocessed Data Sample for use in "modalfrf.m" (2048 samples per window)

There are three different components to consider when evaluating an FRF plot: magnitude, phase, and coherence. Magnitude and phase, when used together, are a great indicator of the frequencies at which resonances exist in a system. Magnitude is essentially the intensity of the response and, when shown in the frequency domain, allow for easy identification of a resonance mode. Phase is a value that exists between -180° and 180° and is also useful for identification of a resonances as the response will lag the input by 90°. Coherence is a value between 0 and 1 that is essentially used to show the goodness of the test across the frequency domain. Values near 1 indicate good repeatability and values close to 0 indicate errors in data collection. Figure 6 shows how the resonance for an idealized SDOF system would look in with respect to magnitude and phase.

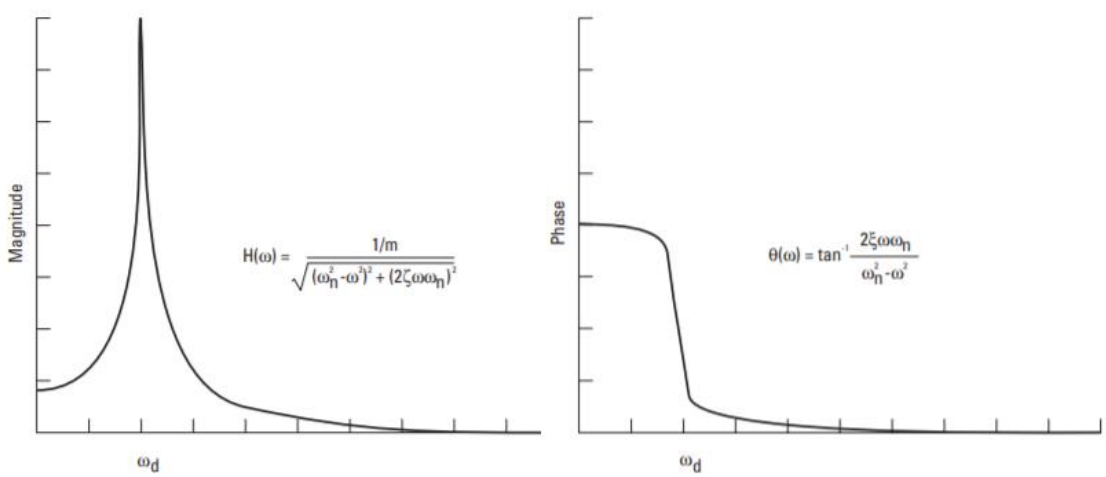

Figure 6: Magnitude and Phase for Resonance of a SDOF System

2.2: Long Run Tests

Long tests were designed to wear-in the test bearing as well as characterize the steady state nature of the Bearing Test Rig under extended operation. The tests also were used to determine the differences between unloaded and loaded scenarios at constant speeds. Tests are carried out such that the motor speed is held constant for four hours. During this time, the Bearing Test Rig is unloaded for the first two hours, then 1500 lb of radial load is

applied for the second two hours. The motor speed is then increased for the next four-hour block to increase the breadth of data.

2.3: Ramp-up Tests

The motivation behind a ramp-up test is to collect vibration data at various motor speeds to identify how vibration signatures change as a function of shaft speed. The test starts by running the Bearing Testing Rig at a shaft speed of 15 Hz with 1500 lb radial load on each test bearing for 30 minutes to heat up the grease in the support bearings. This ensures that the support bearings are warm and well lubricated, while minimizing the risk of skidding in the bearings. Once 30 minutes have passed and the bearing temperatures have reached about 45 °C, the speed is reduced to 5 Hz and data collection begins. The shaft speed is increased by 1 Hz after each data collection period until the final speed of 20 Hz is reached.

2.4: Accelerated Degradation Testing

Before further testing, the test bearing's outer race was seeded with a fault using the brinelling drop-weight fixture shown in Figure 7. This fixture held the bearing's outer race in place, while an impact load was delivered to form a brinell on the test bearing's outer race.

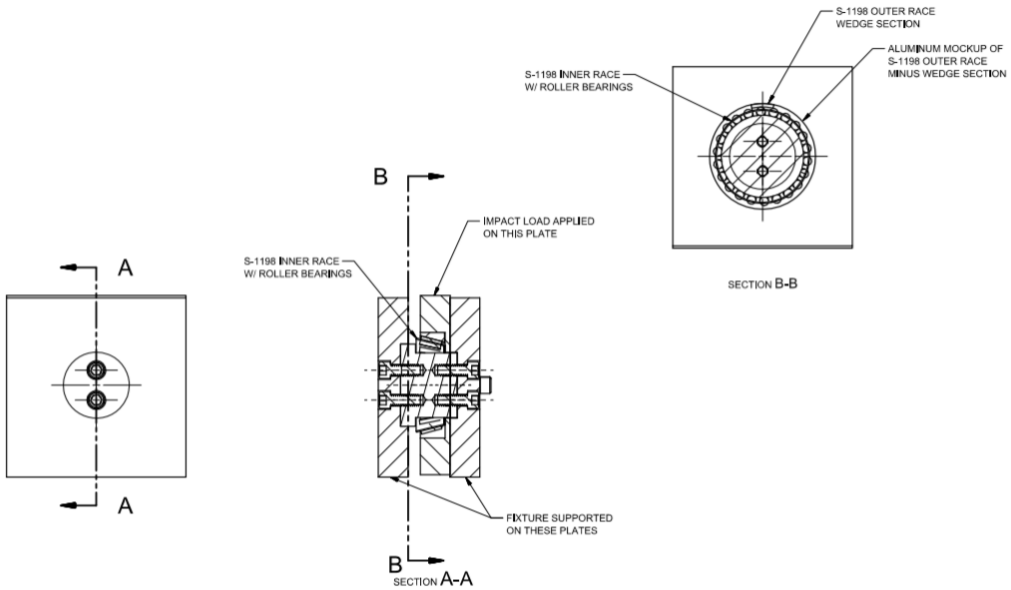

Figure 7: Brinelling Drop-weight Fixture

A progressive loading scheme and initial lubricant dose of 6ml were determined for entering the boundary lubrication regime. Lubricant was added using a syringe then the machine was brought up to an operating speed of 20 Hz. Incremental loads of 2,500 lb, 4,000 lb, and 6,000 lb were applied to the bearing. Each time, the bearing was allowed to

reach a constant temperature before applying an additional load. These temperatures were 40°C, 60°C, and 75°C, respectively. The bearing is rated for 6,340 lb. Once the bearing was at 75°C, the bearings were overloaded to 8,000 lb. The temperature rise will level off until boundary lubrication is exited, which can be observed by a far more rapid increase in temperature.

Results:

This section will feature visual representations of collected data as well as highlight the features of importance in each test.

3.1: Frequency Response Results

Initially, the Bearing Test Rig was on isolation pads, while the motor was fixed to the table. This configuration showed a clean FRF with respect to the coherence, however, strong resonances were observed between the rig and the motor. Figure 8 shows the FRF in the Y-direction, parallel to the earth and normal to the shaft of the rig. The data were recorded at a rate of 10,240 Hz using a wax-mounted, single-axis accelerometer.

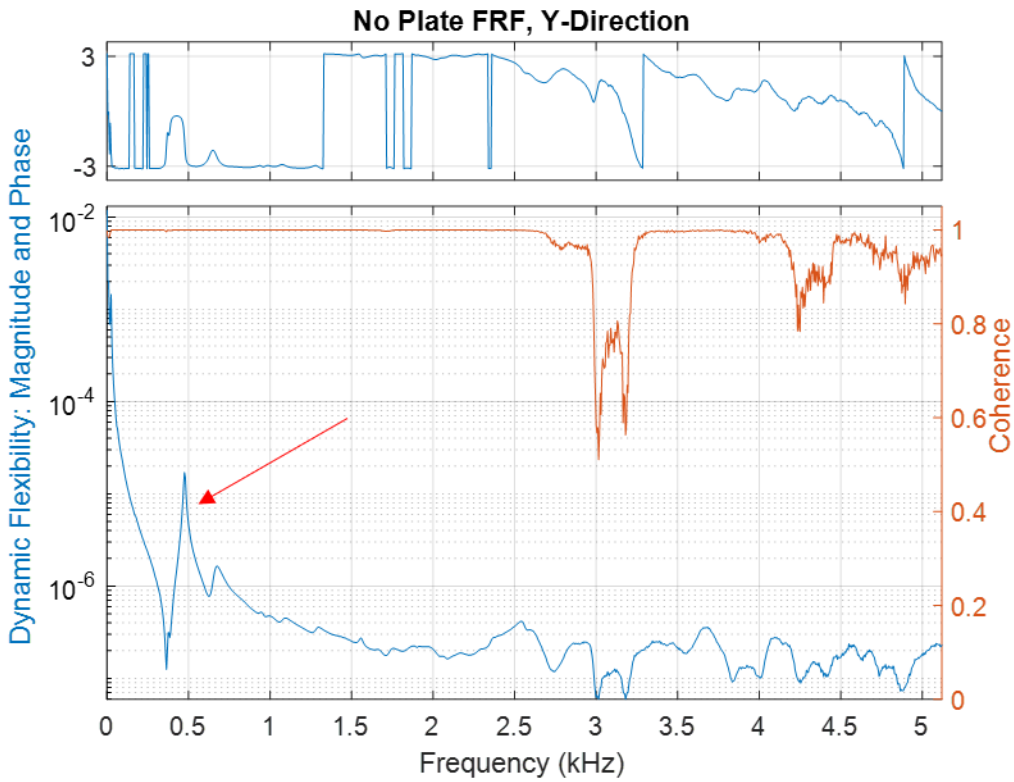

Figure 8.Frequency Response Function, No Plate, Y-Direction

Figure 8 shows good coherence up to 2700 Hz. A single, strong resonance can be seen at approximately 500 Hz. To reduce the effects of this resonance, the motor and Bearing Test Rig were mounted on a common plate to provide additional stiffness to the system. Figure

9 shows the results for the FRF when the motor and Bearing Test Rig were attached to a common plate.

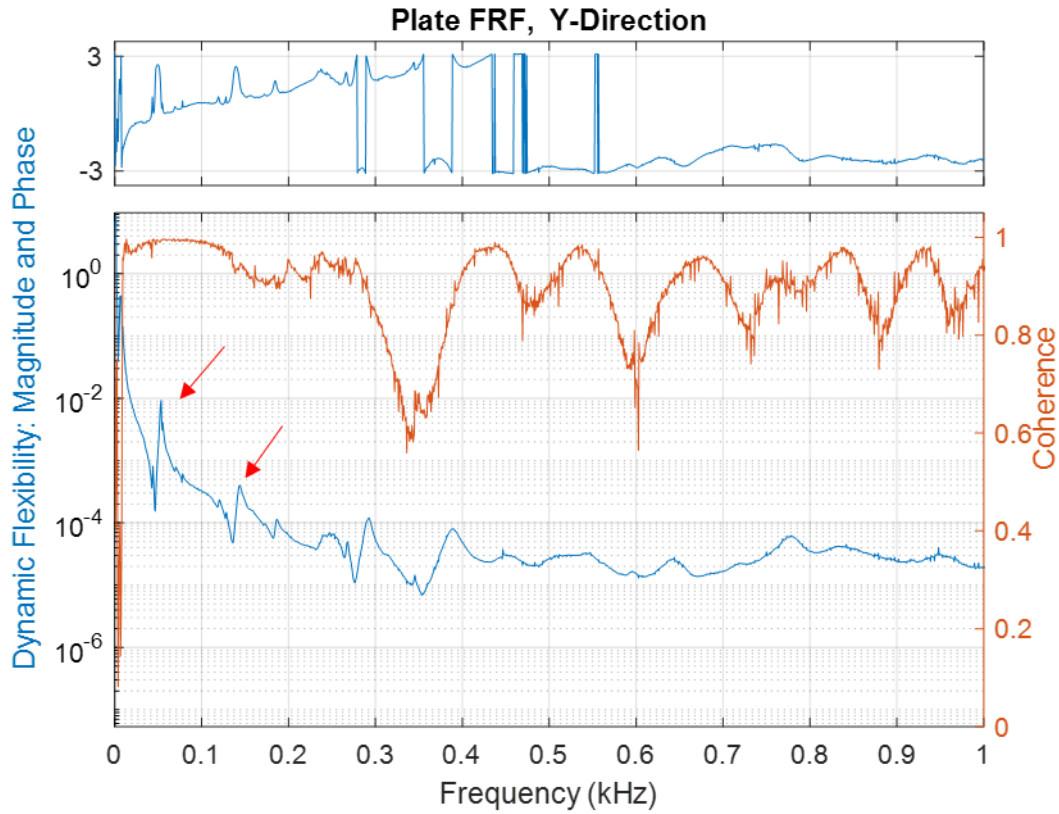

Figure 9. Frequency Response Function, Plate, Y-Direction

With the common plate, notable resonances can be observed at 50 and 150 Hz. While the resonances have a higher magnitude, the additional stiffness of the plate suppresses these resonances from occurring when operation speeds keep the bearing fault frequencies away from 50 Hz. While the coherence was near 1 at the resonances, higher frequencies show a drop in the coherence. This is also due to the additional stiffness introduced by the common plate as it provides a more complex geometry and additional pathways for vibrations to travel. Operation of the bearing test rig was found to have quieter operation in the case where the motor and the Bearing Test Rig were fixed to a common plate. In the case where the Bearing Test Rig was free from the motor, the 500 Hz vibration would occur as part of normal operation as it was excited by the elasticity of the drive belt, raising the overall RMS of the signal regardless of operating speed.

3.2: Long Run Results

The long run consisted of two different shafts speeds in combination with two different loads over several hours. This test was used to wear-in and characterize the bearings under different loading schemes. Figure 10 shows the vibration spectra for two shaft speeds: 6 Hz for samples 1 to 18 and 10 Hz for samples 19 to 37. A 1500 lb load was placed on the

bearings for samples 9-18 and samples 28-37, respectively. Each combination was ran for two hours.

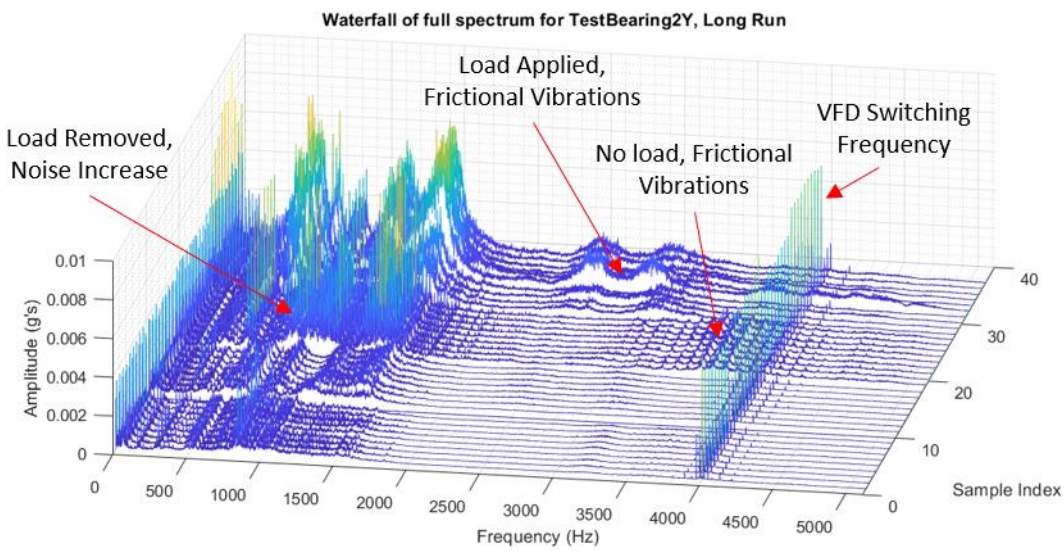

Figure 10: Evidence of Skidding, Long Run

A strong peak at 4000 Hz is observed throughout the spectra. This is due to the switching frequency in the VFD. This peak was later minimized through a sine wave filter, located between the VFD and motor, and grounding of the rig. A large increase in noise is seen in the spectra at index 19, when load was taken off of the bearings and the motor speed was increased to 10 Hz. Most of the increase in noise occurs in the 500-1500 Hz range, while frictional vibrations began to be observed in the 3000-5000 Hz range. When the load was reapplied at index 28, an increase in noise can be seen in the 2500-3500 Hz range. There is a rise in the noise floor with peaks spaced at the bearing outer race fault frequency, which points to signs of bearing skidding (Institute 2019). This skidding might be caused if the races were not sufficiently pressed there. The forward force from the inner race would not be enough to overcome the resistance from the cage causing the rollers to skid. Disassembling the Bearing Test Rig confirmed the existence of mechanical looseness in an adjacent support bearing through the discovery of a loose bearing lock nut. This bearing lock nut was used to press the inner race into the rollers and outer race.

3.3: Ramp-Up Results

This test is used to help differentiate the Bearing Test Rig's structural resonances from dynamic bearing frequencies. Figure 11 shows the vibration spectra from one such test as a waterfall plot.

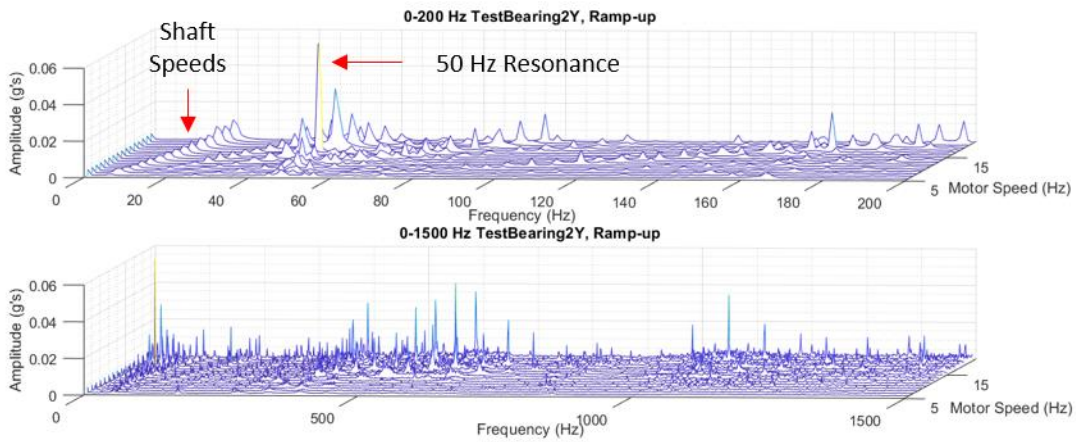

Figure 11: Ramp-up Test Results, Y-direction

In the top plot, the frequencies can be seen increasing as a function of shaft speed, which can be observed by following the first peak in each spectrum. Another notable feature of the top plot is the strong peak seen around 50 Hz. This is a result of a bearing frequency resonating with a structural resonance of the Bearing Test Rig. In the lower plot, additional noise in the spectrum can be seen at the higher frequencies. This was determined to be the onset of skidding due to mechanical looseness as the "self-locking" bearing lock nuts began to loosen. Further evidence of can be seen in the results for the long-run test that took place a few days later. A peak at 4000 Hz that corresponds to the switching frequency of the motor variable frequency drive (VFD) was the only significant peak above 1500 Hz. This peak was seen during the long run in Figure 10.

3.4: Accelerated Degradation Testing Results

As the approach to boundary lubrication is being made, temperature will level off for quite some time around 90-100°C. During this time, the oil within the bearing provides enough lubrication to keep the contact surfaces in elastohydrodynamic lubrication, while the lubricant slowly drips out. Eventually boundary lubrication will be achieved, but the indicator to observe is when the regime is exited, and dry contact begins to take place. This is observed when the temperature begins to climb again as shown by the white line for Test Bearing 1 temperature in Figure 12.

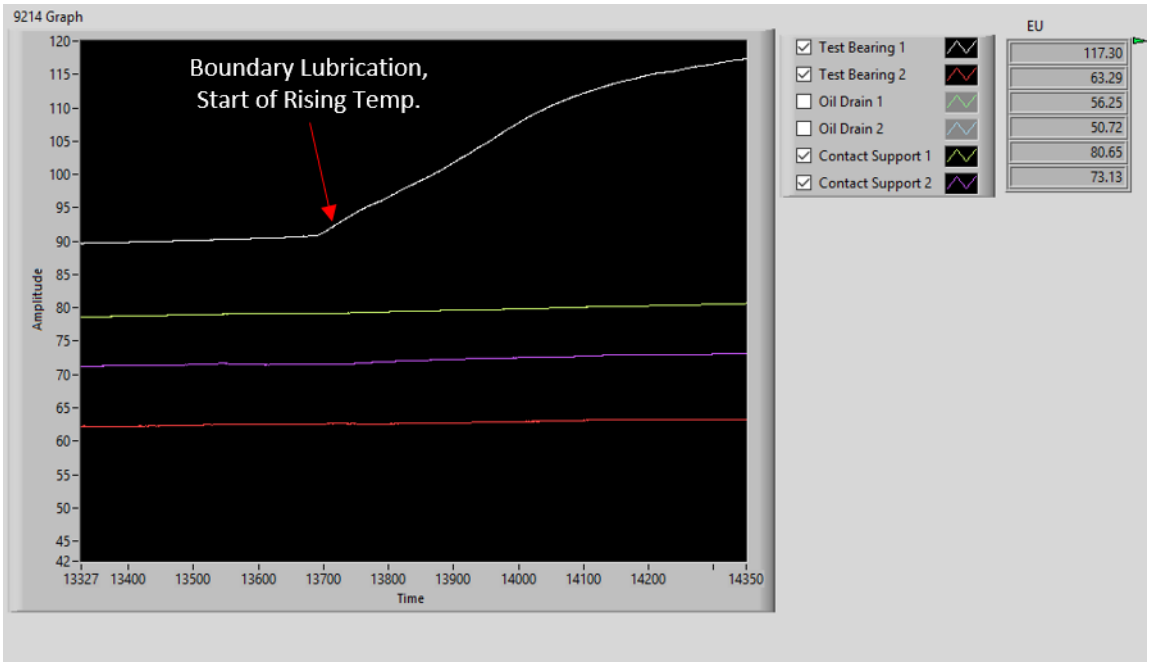

Figure 12.Bearing Temperature, Boundary Lubrication Indication

Further testing is to be carried out to determine the volume and frequency of oil additions to maintain the boundary lubrication conditions for extended runs where bearing degradation will occur. Oil samples will be extracted to determine fluid properties, contamination, and wear debris.

Ongoing work:

Bearings will be monitored inside a wheeled land vehicle's differential to provide realistic data and noise that would only be apparent inside an actual system. A differential is a key component of the drive train in a vehicle. This system allows the rotational speed of one wheel to vary from the other. This is useful during a turn, where the outer tire needs to rotate faster than the inner tire. The carrier bearings inside the differential will be monitored through vibration analysis, while samples will be regularly taken from the splash lubrication system inside the differential.

The test plan for the differential setup is a multistep process. First, the bearing of interest in brinelled using the brinelling drop-weight fixture. The bearing is then monitored and accelerated to a known level of degradation under boundary lubrication. The bearing is inserted into the differential where it is monitored in-situ. The bearing is removed from the differential and again accelerated under boundary lubrication conditions. This process of degradation acceleration then in-situ monitoring is repeated until bearing failure. Oil samples are taken throughout this process during each step. Once a population of bearings have failed, work will begin on creating accurate and robust prognostic models from actual run-to-failure data.

References:

Administration, National Aeronautics and Space. 2019. 'Prognostic Center Data Repository', Accessed Jan 24. https://ti.arc.nasa.gov/tech/dash/groups/pcoe/prognostic-data-repository/.

Aeroshell Turbine Engine Oils. 2012.

Hironaka, S. 1984. 'Boundary Lubrication and Lubricants', *Three Bond Technical News,* July.

Institute, Mobius. 2019. 'Rolling element bearings: Rolling elements skidding', Mobius Institute - Reliability Improvement & Vibration Analysis Training And Certification Per ISO 18436, Accessed Jan 25. https://www.mobiusinstitute.com/site2/item.asp?LinkID=8016&iVibe=1&sTitle=Rolling%20element%20bearings.

James C. Robinson, Meredith Christman. 2018. 'Vibration Monitoring of Paper Mill Machinery', *Sensors for Machinery Health Monitoring*.

'Mobil 1TM Synthetic Gear Lube LS | MobilTM Motor Oils.'. Accessed 11-Jan-2019. https://mobiloil.com/en/gear-lubricants/mobil-1-synthetic-gear-lube-ls.

Nectoux, Patrick, Rafael Gouriveau, Kamal Medjaher, Emmanuel Ramasso, Brigitte Chebel-Morello, Noureddine Zerhouni, and Christophe Varnier. 2012. "PRONOSTIA: An experimental platform for bearings accelerated degradation tests." In *IEEE International Conference on Prognostics and Health Management, PHM'12.*, 1-8. IEEE Catalog Number: CPF12PHM-CDR.

Snow, Dennis A. 2001. *Plant engineer's reference book* (Elsevier).

Solutions, Integrated Reliability. 2019. 'Bearing Skidding', Accessed 2-13-2019. https://www.lubrication.com.au/case-studies/bearing-skidding/.

Team, U.S. Joint Helicopter Safety Implementation. 2013. 'Health and Usage Monitoring Systems Toolkit', International Helicopter Safety Team. http://www.ihst.org/portals/54/toolkit_hums.pdf.

Technologies, Agilent. 1997. "The Fundamentals of Modal Testing." In, 14-29. Hewlett-Packard Co.